JCB Report

Different degrees of lever arm rotation control myosin step size

Danny Köhler,[1] Christine Ruff,[2] Edgar Meyhöfer,[2] and Martin Bähler[1]

[1]Institute for General Zoology and Genetics, Westfälische Wilhelms-University, 48149 Münster, Germany
[2]Molecular and Cellular Physiology, Medical School Hannover, 30625 Hannover, Germany

Myosins are actin-based motors that are generally believed to move by amplifying small structural changes in the core motor domain via a lever arm rotation of the light chain binding domain. However, the lack of a quantitative agreement between observed step sizes and the length of the proposed lever arms from different myosins challenges this view. We analyzed the step size of rat myosin 1d (Myo1d) and surprisingly found that this myosin takes unexpectedly large steps in comparison to other myosins. Engineering the length of the light chain binding domain of rat Myo1d resulted in a linear increase of step size in relation to the putative lever arm length, indicative of a lever arm rotation of the light chain binding domain. The extrapolated pivoting point resided in the same region of the rat Myo1d head domain as in conventional myosins. Therefore, rat Myo1d achieves its larger working stroke by a large calculated ~90° rotation of the light chain binding domain. These results demonstrate that differences in myosin step sizes are not only controlled by lever arm length, but also by substantial differences in the degree of lever arm rotation.

Introduction

Myosins constitute a large superfamily of actin-based motors (Mooseker and Cheney, 1995; Mermall et al., 1998). They use the chemical energy of ATP hydrolysis to generate directed movement along actin filaments. Crystallographic data, mostly from conventional myosins, indicate that small conformational changes induced in the myosin head domain by different nucleotide states and binding to F-actin are transmitted to a converter domain that undergoes a large rotational movement (Dominguez et al., 1998). Attached to the converter is the elongated light chain binding domain that acts as a rigid lever arm (Rayment et al., 1993; Whittaker et al., 1995; Uyeda et al., 1996; Suzuki et al., 1998; Houdusse et al., 2000; Shih et al., 2000). The light chain binding domain of different myosins differs in length, as it consists of a variable number of IQ motifs that represent binding sites for calmodulin or calmodulin-related EF-hand protein light chains. The step size of conventional class II myosins and of the processive myosin Va has been demonstrated to depend in a linear fashion on the length of the light chain binding domain (Warshaw et al., 2000; Ruff et al., 2001; Purcell et al., 2002).

However, a comparison of reported step sizes for chicken smooth muscle myosin II, *Dictyostelium discoideum* myosin II, chicken myosin 1a (brush border myosin I), rat myosin 1b, myosin V, and myosin VI revealed that they are not directly related to the proposed lever arm length (Veigel et al., 1999, 2002; Warshaw et al., 2000; Rock et al., 2001; Ruff et al., 2001; Tanaka et al., 2002). Therefore, to explain these different myosin step sizes, either one or more determinant in addition to lever arm length or a completely different mechanism, as proposed by Yanagida and coworkers (Kitamura et al., 1999; Tanaka et al., 2002), have to be invoked. A comparison of the step sizes of different myosins and an analysis of how they are controlled will lead to the identification of the determinants for these differences. Such experiments should also resolve the ambiguity about the role of the light chain binding domain as lever arm.

Rat myosin 1d (Myo1d),* formerly called myr 4, belongs to a still poorly characterized myosin I subclass (Bähler et al., 1994). Mammalian Myo1d has been implicated to play a role in the endocytic pathway at a step between the early endosome and the recycling endosome (Huber et al., 2000). It consists of a myosin head domain, a light chain binding domain

Address correspondence to Martin Bähler, Institute for General Zoology and Genetics, Westfälische Wilhelms-University, Schlossplatz 5, 48149 Münster, Germany. Tel.: 49-251-83-23874. Fax: 49-251-83-24723. E-mail: baehler@uni-muenster.de; or Edgar Meyhöfer, Department of Mechanical Engineering, University of Michigan, 2350 Hayward Street, Ann Arbor, MI 48109-2125. Tel.: (734) 647-7856. Fax: (734) 615-6647. E-mail: meyhofer@umich.edu

C. Ruff's present address is European Patent Office, D-80331 Munich, Germany.

E. Meyhöfer's present address is Department of Mechanical Engineering, University of Michigan, Ann Arbor, MI 48109-2125.

Key words: myosin 1d; motor molecule; calmodulin; IQ motif; single molecule measurement

*Abbreviation used in this paper: Myo1d, myosin 1d.

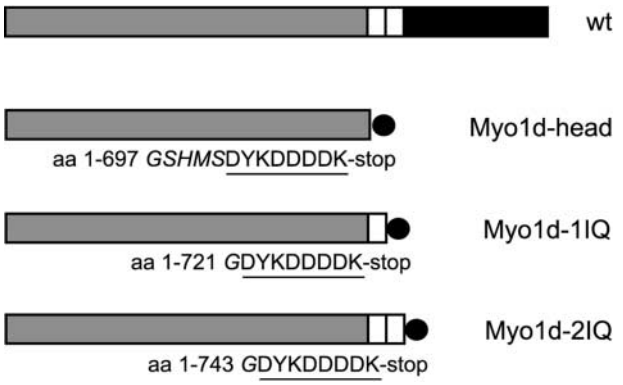

Figure 1. **Schematic representation of the domain organization of wild-type rat Myo1d (wt) and the three recombinant constructs used in this work.** Motor domains (gray), IQ motifs (white), and tail domain (black) are indicated. All recombinant constructs contain a COOH-terminal FLAG-epitope (circle). Amino acids of rat Myo1d, linker residue(s) (italics), and the FLAG-epitope sequence (underlined) included in the three different constructs are given.

with two IQ motifs each binding the Ca^{2+}-sensor protein calmodulin, and a relatively short tail domain (Bähler et al., 1994). Here, we report on the analysis of the mechanical properties of various Myo1d constructs by single molecule measurements. We could show that this motor translocates actin filaments with an unexpectedly large step size due to a large deduced angular rotation (~90°) of its light chain binding domain.

Results and discussion

Biochemical characterization of Myo1d

To investigate whether rat Myo1d is indeed a motor, and if so, whether its step size is determined by the same parameters as in conventional class II myosins, we expressed three recombinant rat Myo1d motors with different numbers of light chain binding sites in HeLa cells (Fig. 1). For ease of purification, all our Myo1d constructs were FLAG-tagged at their COOH termini. Affinity purification yielded virtually pure Myo1d head domain and Myo1d head domains encompassing either one or two IQ motifs (Fig. 2 A). Endogenous calmodulin was copurified with the rat Myo1d head domains containing one or two IQ motifs (Fig. 2 B and Table I). The molar ratios of calmodulin to rat Myo1d were determined to be 1.03 ± 0.05 for Myo1d head-1IQ and 1.74 ± 0.15 for Myo1d head-2IQ, respectively. No calmodulin was copurified with the Myo1d head domain that contained no IQ motif (Fig. 2 B). All three constructs exhibited actin-activated ATPase activity. In the absence of actin, the ATPase activities were barely measurable (0.01–0.06 s^{-1}). However, in the presence of actin, the ATPase activities reached V_{max} values of 2–3 s^{-1} with K_M values for actin of 35–40 μM (Table I and Fig. 2 C). Notably, the addition of one or two IQ motifs to the Myo1d head did not significantly change ATPase rates and actin affinities.

Single molecule measurements of Myo1d

Having established that these three Myo1d constructs exhibit biochemical properties of a motor molecule, we tested them for mechanical activities by single molecule measurements using a combined microneedle laser trap system (Ruff et al., 2001). All three constructs were able to produce directed force along actin filaments as monitored by micronee-

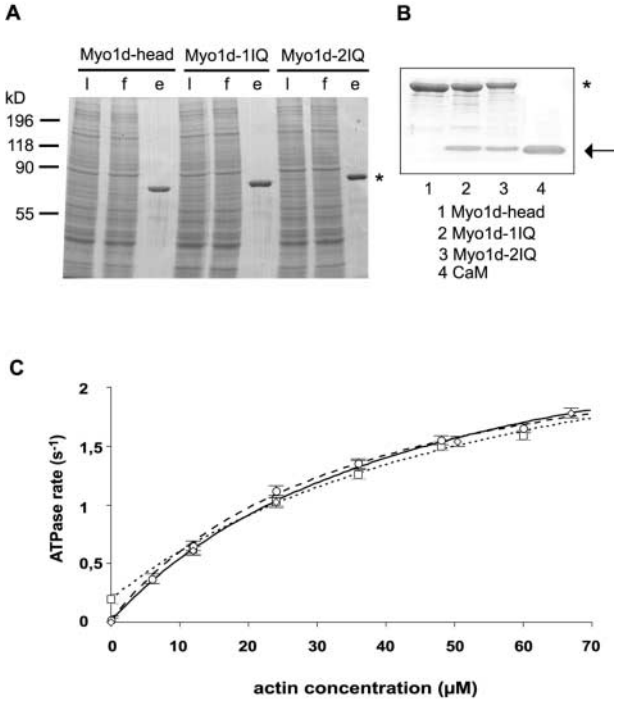

Figure 2. **Purification of recombinant rat Myo1d proteins and analysis of actin-activated ATPase activity.** (A) Cell lysate (l), flow-through of FLAG-column (f), and affinity-purified eluate (e) from each construct were separated on a 7.5% SDS-polyacrylamide gel and stained by Coomassie blue. Molecular weights are indicated on the left, constructs of rat Myo1d are given on top. The asterisk highlights the myosin heavy chains. (B) Coomassie-stained gradient gel of purified rat Myo1d proteins demonstrating the copurification of calmodulin. The asterisk highlights the myosin heavy chains. The arrow marks the position of calmodulin as determined by the migration of purified calmodulin (lane 4). (C) Steady-state ATPase rates for all purified rat Myo1d proteins as a function of actin concentration. Data points for Myo1d-head (circles, dashed line), Myo1d-1IQ (diamonds, straight line), and Myo1d-2IQ (squares, dotted line) were fitted to a hyperbolic equation.

Table I. **Biochemical data and step sizes of recombinant Myo1d**

	Myo1d-head	Myo1d-1IQ	Myo1d-2IQ
Molecules CaM per heavy chain[a]	0	1.03 ± 0.05	1.74 ± 0.15
Basal ATPase rate [s^{-1}][b]	0.01	0.01	0.06
Actin-activated ATPase rate v_{max} [s^{-1}]	2.6 ± 0.1	3.1 ± 0.2	2.7 ± 0.5
$K_{M,\ actin}$ [μM][c]	38.1 ± 3.2	34.4 ± 10.8	39.6 ± 11.2
Step size [nm] (number of single actomyosin events/ number of actin filaments)	4.9 ± 0.21 (1,974/11)	9.3 ± 0.22 (1,883/11)	13.9 ± 0.15 (896/5)

[a]Values were obtained from densitometric analysis as described in Materials and methods.
[b]Basal ATPase rates are myosin activities in the absence of actin.
[c]Actin concentration at half the maximum rate in the presence of 2 mM ATP.

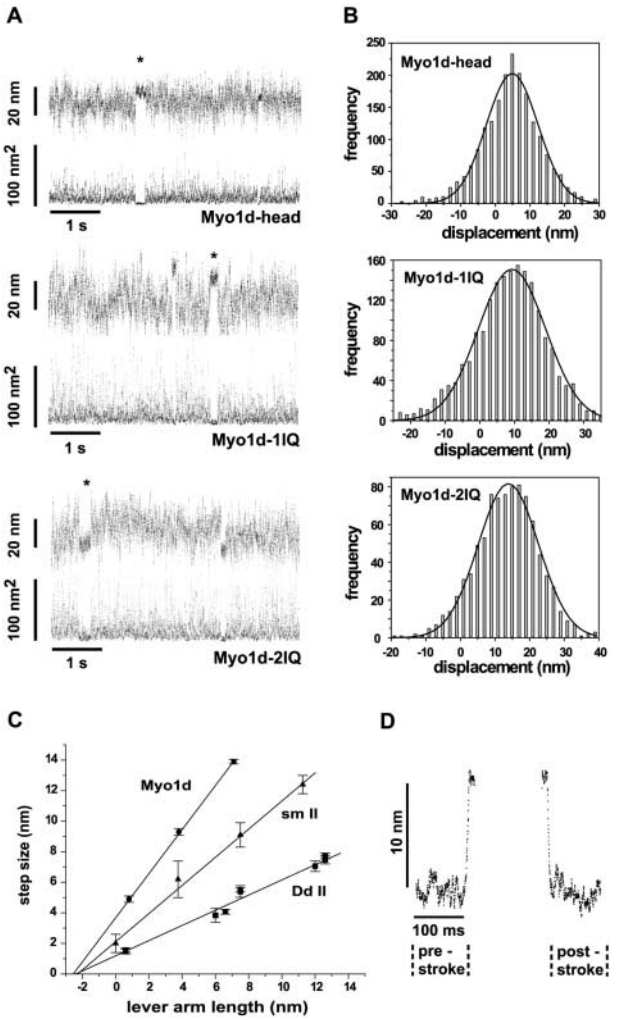

Figure 3. **Single molecule step sizes of different rat Myo1d constructs.** (A) Displacement records showing the interaction of a single actin filament with recombinant rat Myo1d molecules encompassing variable numbers of light chain binding sites. For each construct, representative traces of raw needle displacements (top trace) and the corresponding running variance recordings (bottom trace) are shown. During the attachment of a motor molecule, the fluctuation of the bead–filament–needle complex is significantly reduced. The records contain many actomyosin interactions of variable length; in each panel we highlighted one interaction by an asterisk. Attachments occur over the entire range of the free needle positions. According to Molloy and coworkers (Molloy et al., 1995), the positions of several events show a Gaussian distribution shifted for a distance equivalent to the step size. (B) Distribution of events for the different constructs, summarizing the (oriented) results of several measurements. (C) Step sizes are plotted against the putative lever arm lengths of the various rat Myo1d proteins (circles). The putative lever arm length was calculated by assuming an α-helical conformation of the light chain binding domain. The corresponding solid line represents the best fit of a linear regression analysis. For comparison, previously reported data of *D. discoideum* myosin II (Dd II, squares; Ruff et al., 2001) and chicken smooth muscle myosin II (sm II, triangles; Warshaw et al., 2000) are also included. The Myo 1d-head construct possesses a COOH-terminal linker of five amino acids that contributes 0.75 nm to the putative lever arm helix. FLAG-tag of Myo1d and $(His)_8$-tag of *D. discoideum* myosin II (Ruff et al., 2001) are not included in this calculation. (D) Analysis for possible substep displacements. Example showing synchronized and averaged records from the interaction of a single actin filament with Myo1d-1IQ ($n = 69$). We detect no substeps with this analysis, as the average beginning and ending positions differ by <1 nm. In agreement with the histogram analysis, this analysis predicts a step size of just below 10 nm.

dle displacements that were correlated with a reduction in running variance of the microneedle to below 5 nm^2 (Fig. 3 A), proving that rat Myo1d is a bona fide motor molecule. Interestingly, the Myo1d motor constructs showed step sizes about three times as large as those reported previously for conventional class II myosins (Molloy et al., 1995; Mehta et al., 1997; Ruff et al., 2001). The step size of the Myo1d head was 4.9 nm, the step size of the Myo1d head-1IQ was 9.3 nm, and finally, the step size of the Myo1d head-2IQ was 13.9 nm (Fig. 3 B and Table I). Only one step per power stroke was resolved when records from all three constructs were analyzed for step amplitudes at the start and end of the interactions with a time resolution of better than 5 ms (Fig. 3 D). For all three constructs, we observed differences at the beginning and end of average records of <1 nm, suggesting that Myo1d either moves in a single step, or the substeps follow in rapid succession (<5 ms separation) that we could not detect them. This distinguishes the movement of rat Myo1d from the movements observed for chicken Myo1a and rat Myo1b, which moved in two discrete steps per power stroke (Veigel et al., 1999).

The step sizes of rat Myo1d constructs increased linearly with the number of light chain binding sites and their putative lever arm lengths (Fig. 3 C), indicating that the light chain binding domain serves as a lever. Calculation of the position of the pivot point within the head of rat Myo1d revealed that it is located at virtually the identical position as in the heads of class II myosins (Fig. 3 C). This result strongly suggests that the large step size of rat Myo1d was not caused by the movement of additional regions within the head domain or by a movement at the actomyosin interface. Therefore, the large step size of the rat Myo1d must be due to a large rotation of the lever. If we assume that the step displacements generated by Myo1d and myosin II are entirely based on the rotation of the light chain binding domain about a single pivot point, then we calculate an angular rotation for Myo1d of ~90°. In comparison, the lever of Dd myosin II swivels only by 30° to achieve the measured step sizes (Ruff et al., 2001). These differences in the degree of lever arm rotation between myosins are unlikely to be caused by differences in the attachment to the surface. Identical step sizes were determined for rat Myo1d constructs and Dd myosin II, irrespective of a direct adsorption to the surface or adsorption to an antibody directed against an epitope engineered at the very COOH termini (unpublished data; Ruff et al., 2001). In all myosins tested, step size was linearly related to the putative lever arm length, indicating that there were no restrictions in movement of the head and lever arm in the adsorbed molecules analyzed.

A comparison of crystal structures of class II myosin motor domains in different nucleotide states revealed four major subdomains (NH_2-terminal region, lower 50-kD domain, upper-50 kD domain, and converter) that are rearranged relative to each other by three flexible loops or "joints," termed switch II, relay, and SH1 helix, respectively

(Houdusse et al., 1999). We propose that subtle differences in either of the flexible loops will cause differences in the movement and rotation of the converter and the extended α-helix of the attached light chain binding domain. Indeed, a recently reported crystal structure of a class I myosin, *D. discoideum* myosin-IE, showed that the overall structure of the motor domain is almost identical to myosin II and that subtle differences occur in loop regions connecting the main structural elements. Due to differences in the relay loop, the lever arm position in the prepower stroke state extended ~30° further up toward the pointed end of the actin filament than in myosin II (Kollmar et al., 2002). The movement of the Dd myosin-IE lever arm from the pre-power stroke position found in the crystal structure to a similar post-power stroke position as observed in crystal structures of class II myosins (Fisher et al., 1995; Houdusse et al., 1999, 2000) would result in an ~90° rotation along the longitudinal axis of the actin filament. These observations strongly support our model of a large angular rotation during the power stroke of Myo1d.

As recently shown, step size measurements for processively moving myosins include, in addition to the working stroke, a diffusive movement to the next preferred myosin binding position (target zone; Rock et al., 2001; Veigel et al., 2002). In the backward moving myosin VI, which contains a unique 53-aa residue insert between the converter and light chain binding domain, this diffusive component appears to be quite large (Rock et al., 2001; Spudich and Rock, 2002). Although details of the processive movements of myosin V and VI still need to be worked out, we believe that these observations are not in conflict with the lever arm role of the light chain binding domain of myosins as suggested by Tanaka et al. (2002).

We conclude that the degree of lever arm rotation varies considerably among different myosins, and that it is an important determinant for myosin step size. Both determinants together, lever arm length and degree of lever arm rotation, are sufficient to explain the reported ATP-induced conformational changes or working strokes (often referred to as step size).

Materials and methods

Plasmid construction

The rat Myo1d head-FLAG cDNA encoding aa 1–697 of Myo1d followed by linker amino acids GSHMS and the FLAG-tag sequence DYKDDDDK was cloned into the expression vector pIRES-hygromycin (CLONTECH Laboratories, Inc.). The pIREShyg plasmid was modified previously to encompass SmaI, NheI, Bsu36I, and EcoRV restriction sites between the BamHI and BstXI restriction sites. Myo1d head-FLAG cDNA was cloned into the SmaI and EcoRV restriction sites in a two-step process. A 3′ fragment was amplified by PCR and subcloned into pIREShyg. The remaining 5′ fragment was excised from pBSK-Myo1d and ligated. To construct the Myo1d head-1IQ-FLAG plasmid (encompassing aa 1–721 of Myo1d followed by a glycine residue and the FLAG epitope) and the Myo1d head-2IQ-FLAG plasmid (encompassing aa 1–743 followed by a glycine residue and the FLAG epitope), 3′ fragments were amplified by PCR and inserted into the BstEII/BstXI sites of the Myo1d head-FLAG construct. PCR fragments were verified by sequencing.

Cell culture

HtTA-1 HeLa cells (Gossen and Bujard, 1992) were cultured at 37°C and 5% CO_2 in DME supplemented with 10% FCS, 100 U/ml penicillin, and 100 μg/ml streptomycin. Cells were transfected by calcium phosphate precipitation of plasmid DNA. Single colonies were isolated after selection in 200 μg/ml hygromycin for 2 wk and were subcloned. Cells were analyzed for Myo1d construct expression by immunoblotting with the rat Myo1d antibody SA 522. Selection by hygromycin was maintained continuously.

Protein purifications

For purification of recombinant proteins, cells were grown in 10–20 culture dishes (Ø 150 mm) to near confluency. Cells were washed twice with PBS (150 mM NaCl, 3 mM Na_2HPO_4, and 1.5 mM KH_2PO_4) and collected by scraping. They were lysed in lysis buffer (150 mM NaCl, 20 mM Hepes, pH 7.4, 2 mM $MgCl_2$, 1 mM EGTA, 0.5% Triton X-100, 2 mM ATP, 0.1 mg/ml Pefabloc®, 0.01 mg/ml leupeptin, and 0.02 U/ml aprotinin) for 1 h on ice, and cleared by centrifugation at 40,000 *g* for 30 min followed by ultracentrifugation at 170,000 *g* for 45 min. The supernatant was mixed with 1 ml FLAG-antibody agarose (Sigma-Aldrich) and incubated for 2 h at 6°C. Agarose beads were washed twice with buffer WP containing 50 mM KCl, 10 mM Hepes, pH 7.4, 2 mM $MgCl_2$, 1 mM EGTA, 1 mM 2-mercaptoethanol, and 2 mM NaN_3. Bound protein was eluted by supplementing buffer WP with 125 μg/ml soluble FLAG peptide (Sigma-Aldrich). The eluted protein was dialyzed for 36 h with two buffer changes against buffer WP. Purified proteins were sometimes concentrated using microcon filters (cut-off 10 kD; Millipore). Densitometric analysis of Coomassie-stained protein bands on SDS gels was performed with a laser densitometer (Ultrascan; LKB). Values represent the mean from at least three different preparations. Purified calmodulin was purchased from Sigma-Aldrich. Actin was purified from rabbit skeletal muscle as described elsewhere (Pardee and Spudich, 1982).

ATPase assays

Steady-state ATPase activities at 37°C were determined by quantitation of P_i release from γ[^{32}P]ATP as described previously (Stöffler and Bähler, 1998). Assay mixtures contained 30 mM KCl, 10 mM Hepes, pH 7.4, 2 mM $MgCl_2$, 2 mM ATP, 2 mM EGTA, 1 mM 2-mercaptoethanol, 2 mM NaN_3, and various actin concentrations. Purified Myo1d constructs were used in a concentration range between 25 and 200 nM. Kinetic values represent averaged numbers derived from at least three different preparations.

Step size measurements and data analysis

The combined microneedle laser trap transducer that was used to measure step sizes has been described in detail previously (Ruff et al., 2001). In brief, the actin filament is pulled taught between a small latex bead (d = 1.0 μm) captured in a laser trap and the tip of a fine glass microneedle. The needle serves as sensor for the transient interactions of the filament with single motor molecules attached to the substrate. All single molecule measurements were performed at 23°C (± 0.5°C) in 25 mM imidazol, pH 7.4, 25 mM KCl, 1 mM EGTA, 4 mM $MgCl_2$, 1 μM ATP, 10 mM DTT, 100 μg/ml glucose oxidase, 18 μg/ml catalase, and 3 mg/ml glucose. Recombinant rat Myo1d proteins were adsorbed directly to the nitrocellulose-coated surface of the recording chamber using 10-min incubations. Alternatively, they were coupled via an anti-FLAG mAb (M2; Sigma-Aldrich) to the nitrocellulose surface. In these experiments, nonspecific binding was reduced by blocking the surface with BSA.

Data analysis was performed with custom-written software as described in detail previously (Ruff et al., 2001). The running variance was calculated with a 10-ms window, and individual events were identified based on the reduction of the variance. The positions of all events relative to the zero position of the free needle were plotted in a histogram and oriented. Measurements obtained with several actin filaments and different protein preparations were pooled to obtain large datasets for each construct. To establish if Myo1d moves in discrete substeps, like Myo1a, we followed the analysis approach outlined by Veigel et al. (1999), and determined the average position at the beginning and end of the actomyosin interactions. In brief, we detected the beginning and end of individual actomyosin interactions by monitoring the reduction in the variance of a 5-ms running window, and averaged many record segments at the beginning (consisting of 100 ms before and 15 ms into the detected interaction) and separately averaged the end of many individual actomyosin interactions (last 15 ms of the actomyosin event and the 100 ms segment directly after the detachment of myosin). If the step displacement is generated in distinct substeps, positions of synchronized, average beginning and ending event positions will differ. The analysis is principally limited by the bandwidth of the microneedle laser trap detector and the ability to precisely determine the time of the start and end of each interaction in the thermal fluctuations of free actin–microneedle laser trap complex. For the experiments and analysis reported here, we can confidently resolve substeps separated by >3–5 ms.

We thank Susanne Kempter and Margrit Müller for skillful technical assistance.

This work was supported by grants of the Deutsche Forschungsgemeinschaft (BA1354/6-1 to M. Bähler, and ME1414/4-2 to E. Meyhöfer).

Submitted: 4 December 2002
Revised: 11 March 2003
Accepted: 11 March 2003

References

Bähler, M., R. Kroschewski, H. Stöffler, and T. Behrmann. 1994. Rat myr4 defines a novel subclass of myosin I: identification, distribution, localization, and mapping of calmodulin-binding sites with differential calcium sensitivity. *J. Cell Biol.* 126:375–389.

Dominguez, R., Y. Freyzon, K.M. Trybus, and C. Cohen. 1998. Crystal structure of a vertebrate smooth muscle myosin motor domain and its complex with the essential light chain: visualization of the pre-power stroke state. *Cell.* 94: 559–571.

Fisher, A.J., C.A. Smith, J.B. Thoden, R. Smith, K. Sutoh, H.M. Holden, and I. Rayment. 1995. X-ray structures of the myosin motor domain of *Dictyostelium discoideum* complexed with MgADP.BeFx and MgADP.AlF4-. *Biochemistry.* 34:8960–8972.

Gossen, M., and H. Bujard. 1992. Tight control of gene expression in mammalian cells by tetracycline-responsive promoters. *Proc. Natl. Acad. Sci. USA.* 89: 5547–5551.

Houdusse, A., V.N. Kalabokis, D. Himmel, A.G. Szent-Györgyi, and C. Cohen. 1999. Atomic structure of scallop myosin subfragment S1 complexed with MgADP: a novel conformation of the myosin head. *Cell.* 97:459–470.

Houdusse, A., A.G. Szent-Györgyi, and C. Cohen. 2000. Three conformational states of scallop myosin S1. *Proc. Natl. Acad. Sci. USA.* 97:11238–11243.

Huber, L.A., I. Fialka, K. Paiha, W. Hunziker, D.B. Sacks, M. Bähler, M. Way, R. Gagescu, and J. Gruenberg. 2000. Both calmodulin and the unconventional myosin myr4 regulate membrane trafficking along the recycling pathway of MDCK cells. *Traffic.* 1:494–503.

Kitamura, K., M. Tokunaga, A.H. Iwane, and T. Yanagida. 1999. A single myosin head moves along an actin filament with regular steps of 5.3 nanometres. *Nature.* 397:129–134.

Kollmar, M., U. Dürrwang, W. Kliche, D.J. Manstein, and F.J. Kull. 2002. Crystal structure of the motor domain of a class-I myosin. *EMBO J.* 21:2517–2525.

Mehta, A.D., J.T. Finer, and J.A. Spudich. 1997. Detection of single-molecule interactions using correlated thermal diffusion. *Proc. Natl. Acad. Sci. USA.* 94: 7927–7931.

Mermall, V., P.L. Post, and M.S. Mooseker. 1998. Unconventional myosins in cell movement, membrane traffic, and signal transduction. *Science.* 279:527–533.

Molloy, J.E., J.E. Burns, J. Kendrick-Jones, R.T. Tregear, and D.C.S. White. 1995. Movement and force produced by a single myosin head. *Nature.* 378:209–212.

Mooseker, M.S., and R.E. Cheney. 1995. Unconventional myosins. *Annu. Rev. Cell Dev. Biol.* 11:633–675.

Pardee, J.D., and J.A. Spudich. 1982. Purification of muscle actin. *Methods Cell Biol.* 24:271–289.

Purcell, J.T., C. Morris, J.A. Spudich, and H.L. Sweeney. 2002. Role of the lever arm in the processive stepping of myosin V. *Proc. Natl. Acad. Sci. USA.* 99: 14159–14164.

Rayment, I., W.R. Rypniewski, K. Schmidt-Base, R. Smith, D.R. Tomchick, M.M. Benning, D.A. Winkelmann, G. Wesenberg, and H.M. Holden. 1993. Three-dimensional structure of myosin subfragment-1: a molecular motor. *Science.* 261:50–58.

Rock, R.S., S.E. Rice, A.L. Wells, T.J. Purcell, J.A. Spudich, and H.L. Sweeney. 2001. Myosin VI is a processive motor with a large step size. *Proc. Natl. Acad. Sci. USA.* 98:13655–13659.

Ruff, C., M. Furch, B. Brenner, D.J. Manstein, and E. Meyhöfer. 2001. Single-molecule tracking of myosins with genetically engineered amplifier domains. *Nat. Struct. Biol.* 8:226–229.

Shih, W.M., Z. Gryczynski, J.R. Lakowicz, and J.A. Spudich. 2000. A FRET-based sensor reveals large ATP hydrolysis-induced conformational changes and three distinct states of the molecular motor myosin. *Cell.* 102:683–694.

Spudich, J.A., and R.S. Rock. 2002. A crossbridge too far. *Nat. Cell Biol.* 4:E8–E10.

Stöffler, H.-E., and M. Bähler. 1998. The ATPase activity of purified myr 3, a rat myosin I, is allosterically inhibited by its own tail domain and by Ca^{2+}-binding to its light chain calmodulin. *J. Biol. Chem.* 273:14605–14611.

Suzuki, Y., T. Yasunaga, R. Ohkura, T. Wakabayashi, and K. Sutoh. 1998. Swing of the lever arm of a myosin motor at the isomerization and phosphate-release steps. *Nature.* 396:380–383.

Tanaka, H., K. Homma, A.H. Iwane, E. Katayama, R. Ikebe, J. Saito, T. Yanagida, and M. Ikebe. 2002. The motor domain determines the large step of myosin-V. *Nature.* 415:192–195.

Uyeda, T.Q.P., P.D. Abramson, and J.A. Spudich. 1996. The neck region of the myosin motor domain acts as a lever arm to generate movement. *Proc. Natl. Acad. Sci. USA.* 93:4459–4464.

Veigel, C., L.M. Coluccio, J.D. Jontes, J.C. Sparrow, R.A. Milligan, and J.E. Molloy. 1999. The motor protein myosin-I produces its working stroke in two steps. *Nature.* 398:530–533.

Veigel, C., F. Wang, M.L. Bartoo, J.R. Sellers, and J.E. Molloy. 2002. The gated gait of the processive molecular motor, myosin V. *Nat. Cell Biol.* 4:59–65.

Warshaw, D.M., W.H. Guilford, Y. Freyzon, E. Krementsova, K.A. Palmiter, M.J. Tyska, J.E. Baker, and K.M. Trybus. 2000. The light chain binding domain of expressed smooth muscle heavy meromyosin acts as a mechanical lever. *J. Biol. Chem.* 275:37167–37172.

Whittaker, M., E.M. Wilson-Kubalek, J.E. Smith, L. Faust, R.A. Milligan, and H.L. Sweeney. 1995. A 35-Å movement of smooth muscle myosin on ADP release. *Nature.* 378:748–751.